

Development of Abaca Fiber-reinforced Foamed Fly Ash Geopolymer

Ngo, Janne Pauline S.^{1*}, Promentilla, Michael Angelo B.^{1,2}

¹Chemical Engineering Department, De La Salle University, Manila 0922, Philippines

²National Research Council of the Philippines, Taguig, Metro Manila 1631, Philippines

Abstract. The growing environmental and economic concerns have led to the need for more sustainable construction materials. The development of foamed geopolymer combines the benefit of reduced environmental footprint and attractive properties of geopolymer technology with foam concrete's advantages of being lightweight, insulating and energy-saving. In this study, alkali-treated abaca fiber-reinforced geopolymer composites foamed with H₂O₂ were developed using fly ash as the geopolymer precursor. The effects of abaca fiber loading, foaming agent dosage, and curing temperature on mechanical strength were evaluated using Box-Behken design of experiment with three points replicated. Volumetric weight of samples ranged from 1966 kg/m³ to 2249 kg/m³. Measured compressive strength and flexural ranged from 19.56 MPa to 36.84 MPa, and 2.41 MPa to 6.25 MPa, respectively. Results suggest enhancement of compressive strength by abaca reinforcement and elevated temperature curing. Results, however, indicate a strong interaction between curing temperature and foaming agent dosage, which observably caused the composite's compressive strength to decline when simultaneously set at high levels. Foaming agent dosage was the only factor detected to significantly affect flexural strength.

1 Introduction

Sustainability has been an important drive for research for the past years. Increasing consumptions of resources and materials, as well as the immoderately massive generation of waste, has pulled the research and development of modern materials towards greener alternatives. An important factor to consider is the construction industry to which over 40% of the global energy consumption and excessively high quantity of carbon dioxide emission is due [1]. This sector has nonetheless seen growth in demand continually and inevitably. Hence, the development of sustainable construction materials to possibly substitute these commodities and reduce environmental footprint should be sought after. Considering this, one of the most promising and fast-growing research in the past two decades is on geopolymer. Geopolymer, an inorganic binder formed by alkaline activation of solid alumina- and silica-containing materials which are often sourced from industrial waste, has emerged as a potential concrete binder – an alternative to ordinary Portland cement (OPC). Geopolymer production is reported to curb CO₂ emission of traditional cement clinker by 60 to 80% [2]. Moreover, it finds increasing applications in other areas due to its unique properties such as thermal and fire resistance.

Previous studies have reported foamed concrete's brittleness to be unsuitable for bending and squash loads [3]. Fiber reinforcement is commonly employed to enhance mechanical strength by allowing load transfer and crack bridging. Commonly reinforced fibers in cementitious materials include steel and polymeric fibers [4]. The use of natural fiber has recently been explored, particularly for its inherent mechanical properties, low density, low cost, abundance and biodegradability.

1.1 Abaca Fiber

Abaca fiber which is native and abundant in the Philippines is widely used for its commendable mechanical properties and utility for polymer reinforcement. An annual report in 2015 reveals that 70,400 metric tons of the fiber was produced [5]. The large volume of harvested high-grade abaca in turn generates a considerable amount of waste or low-grade fibers [6]. As much as three quarters of the abaca is considered agricultural waste and left in plantations to wither after the high-grade fiber is harvested [7]. About 328.5 million kilograms of abaca waste was reported to be generated annually in 2014. The industry, however, is foreseen to grow even more in the succeeding years. In 2015, it was reported that the outbound shipments of abaca rose by 39.8% from the previous year [8]. In 2016,

* Corresponding authors: janne_ngo@dlsu.edu.ph; michael.promentilla@dlsu.edu.ph

farmers have increased their production of abaca by 5.7% (from 58,665.8 MT to 62,008.6 MT) from the previous year to meet the demand for the crop in the Philippine's export market [9]. It was reported in 2015 that the about 87.7% of the profit gained from abaca came from finished goods such as fabrics, cordage and fiber crafts, while raw abaca fibers accounted for the remaining exports. However, revenue from raw abaca fiber has been tripling year after year [8]. Raw abaca fiber's application in various industries has indeed broadened. As of present, the most common innovative use of abaca-reinforced composites has been in under-floor protection of automotive [10]. With the high volume of agricultural waste involved in this growing industry, it would therefore be advantageous for the environment if these wastes or scrap fibers can be treated and utilized in advanced materials. With that said, this study aims to explore the use of waste abaca fiber as reinforcement in geopolymer with foaming. Particularly, this study aims to develop an abaca-reinforced fly ash geopolymer foamed with hydrogen peroxide (H_2O_2) and to assess its compressive and flexural strength under various fiber loading, H_2O_2 dosage and curing temperature.

1.2 Fiber Pretreatment

Often, reinforcement is employed in order to improve the material's mechanical properties. Fibers are used as load-bearing materials imbedded in another's matrix, thus providing rigidity, strength and flexibility in many cases [4]. The resulting junction is called a composite. Concrete is often reinforced to address premature cracking that develop with shrinkage during the hardening of the paste. This shrinkage, called plastic shrinkage, occurs due to loss of moisture [11]. Fiber reinforcement has been effective preventing crack propagation by bridging cracks and by allowing load transfer. However in some cases, fiber loading can be counterproductive and lead to compressive strength reduction due to factors like improper distribution and weak interfacial interaction. When the fiber acts more as an interference in the matrix than an aid or reinforcement, mechanical properties may become less desirable [11-12].

Stress sharing and transfer between the fiber and the matrix depend on fibre-fibre and fibre-matrix adhesion and interactions. Effective reinforcement relies on compatibility of components. Likewise, incompatibility may only result to decline in mechanical strength and promote deterioration. This has been reported by prior studies to be a disadvantage of natural fibers. Natural fibers typically consist of lignin, pectin, cellulose, hemicellulose, moisture and other compounds such as fats and waxes. It is basically a composite in itself of polymers: cellulose, hemicellulose and lignin [13]. Due to its hydrophilic nature and thus, tendency for water absorption, natural fibers may exhibit weak interfacial bonding with hydrophobic matrix [12, 14-17]. This is often observed in polymer composites. Furthermore,

'swelling' may occur when a hydrophilic fiber within a hydrophobic resin absorbs moisture, making it susceptible to weakening and even deterioration [18]. Consequently, softened fibers will result to reduced strength.

The most economical and well-studied treatment to overcome this disadvantage is alkali treatment [16]. Soaking fibers in alkali solution, commonly sodium hydroxide (NaOH), strips them of impurities which contribute to water absorption and incompatibility. Parts of the amorphous components lignin, hemicellulose and pectin are removed, resulting to smaller fibers with increased effective surface area. The remaining fiber after these components come off will reveal a rough surface, thereby increasing the fiber's resistance to being pulled out of the matrix [16].

2 Methodology

In this study, alkali-pretreatment was performed on the waste abaca as follows: fibers were initially cut to approximately 1 cm strands. A solution of 6 wt% NaOH was prepared from 12M NaOH available. The waste abaca fibers were then submerged in the alkali solution following the proportion 70-80 mg fiber per 100 mL solution for 2 hours. The fibers were subsequently washed with water until they are sufficiently neutralized to about pH 7. Then, the fibers were air-dried for 24 hours. This procedure was reported to yield the best mechanical strength improvement of abaca reinforced in epoxy [17]. **Fig. 1** shows the untreated and treated abaca fibers.



Fig. 1. (a) Untreated and (b) treated abaca fibers

Preparation of geopolymer composites consists of two parts: (1) preparation of alkali activator solution and (2) preparation of the composites. For the alkali activator solution, waterglass to sodium hydroxide solution (WGS/NaOH) was fixed at mass ratio 1.66. The activator solution was mixed thoroughly with a magnetic stirrer. After 15 minutes, 50 wt% hydrogen peroxide was added at 0.16, 0.24 and 0.32 weight % of the fly ash used to the activator solution and mixed for 5 more minutes.

To prepare the specimen with fiber reinforcement, the cut, treated and dried abaca fibers were dry-mixed with sieved fly ash (2mm) to ensure uniform distribution. Fiber loading was designated to 0%, 0.25% and 0.5 wt% of the weight of fly ash used. Meanwhile, the prepared alkali activator was incorporated with the fly ash and

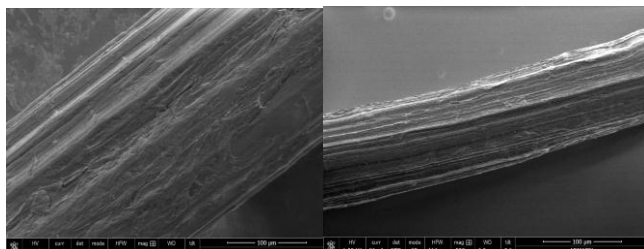
abaca following mass ratio NaOH/FA = 0.2. The slurry was manually mixed first to ensure the desired consistency. Then, the mixture was thoroughly mixed in a mechanical mixer for about 15 minutes until fiber strands were well-distributed and that homogeneity was achieved. The geopolymer paste was then casted on moulds, allowed to dry for 24 hours and removed from the moulds. Samples were then placed in air-tight plastics and cured at various temperatures, 30°C, 52.5°C and 75°C, for 2 hours, followed by 24-hour hardening at room temperature.

Scanning electron microscopy (SEM) images of treated and untreated abaca fibers were taken and analysed. Thermal gravimetric analyses were also performed on the fibers. Subsequently, the prepared geopolymer composites were characterized by SEM image analysis, volumetric weight and water absorption. Finally, compressive strength and flexural strengths of the composites were measured.

3 Results and Discussion

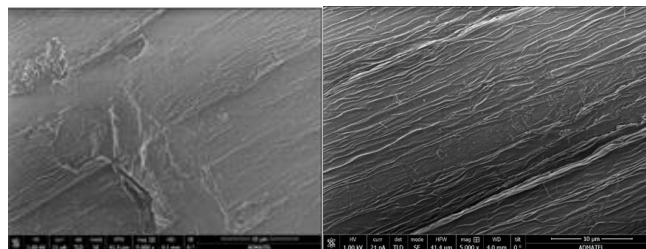
3.1. Scanning electron microscopy (SEM) analysis of abaca

Scanning electron microscopic image analyses were carried out using Field-emission scanning electron microscope (FESEM Dual Beam Helios Nanolab 600i) equipped with electron-dispersive X-ray spectroscopy. Images were taken at accelerating voltage = 2.0 kV and beam current = 43 pA. SEM images of the fiber samples at 500x and 5000x magnification are presented in **Fig. 2**. **Fig. 2a** and **Fig. 2c** shows the untreated fiber whose surface evidently has less uniformity. “Impurities” which could likely be the weak and dislodged hemicellulose are visible. It is observed in **Fig. 2b** and **Fig. 2d** that these impurities were stripped off, revealing a more uniform but rougher surface. After treatment, corrugation on the fiber surface was observed. Corrugation and roughening of the surface indicate a better fiber–matrix interface by virtue of mechanical interlocking. This surface modification indicates higher frictional bond between the two components, which has previously shown to be effective in resisting shear and bending stress



a. untreated, 500x magnification

b. treated, 500x magnification



c. untreated, 500x magnification

d. treated, 500x magnification

Fig. 2. SEM images of waste abaca before and after treatment

3.2. Thermogravimetric analysis (TGA) of abaca

Percent mass loss during the ramp increase in temperature was analyzed using TGA. This analysis allows evaluation of the fiber’s composition. According to previous studies, cellulosic fibers’ thermal decomposition commonly comprises of loss of moisture, degradation of hemicellulose, cellulose and lignin. **Table 1** summarizes this with each component’s degradation temperature [19].

Table 1. Decomposition Temperatures of Natural Fibers’ Components.

Components	Decomposition Temp, °C	T _{max} , °C
Moisture	30 – 100	80
Hemicellulose	160 – 350	245 - 298
Cellulose	240 – 365	335
Lignin	300 – 500	337

Fig. 3 shows the thermograms of both the untreated (a) and treated (b) abaca samples. Meanwhile, **Table 2** summarizes the observed thermal degradation of the untreated and treated abaca samples. T_{max} is defined as the temperature at which the fastest rate of degradation was observed, and it was taken using differential thermogravimetry (DTG). The first stage of decomposition primarily removed free and absorbed moisture from the abaca fibers. For the untreated fiber, decomposition observed between 200°C and 370°C resulted to a mass loss equivalent to 78.2%. T_{max} was observed at 345°C wherein the maximum rate of decomposition was 1.1% per °C. This is mainly accounted to the decomposition of hemicellulose. At the same decomposition stage, the treated fiber experienced a lower % mass loss (71.2%), which indicates its lower hemicellulose content. Beyond this is the onset of the decomposition of cellulose and lignin. This was allowed to proceed up to 900°C, where 87.1% and 79.0% were the measured mass losses for the untreated and treated fiber samples, respectively. This signifies that the treated samples contained lower combined cellulose and lignin content. The untreated fiber’s residual mass was 12.9% while that of the treated sample was 21%. These results

signify that the treatment was able to remove the weak and dislodged components off of the abaca fiber.

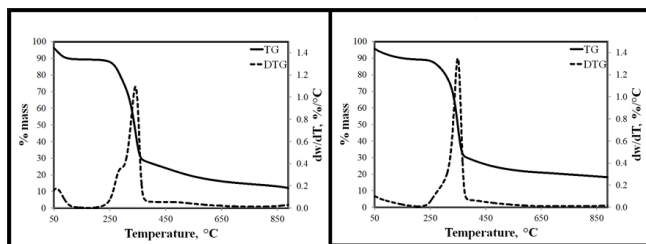


Fig. 3. Thermograms of (a) untreated and (b) treated abaca

Table 2. Observed Decomposition Stages of Abaca Samples

fiber	Decomposition 1			Decomposition 2			% mass loss up 900°C
	T _{max} °C	% mass loss	Rate, %/°C	T _{max} °C	% mass loss	Rate, %/°C	
Raw	62	8.9	0.3	345	78.2	1.1	87.1
Treated	53	7.8	0.1	350	71.2	1.3	79.0

3.3. Density and water absorption of geopolymer composites

The resulting volumetric weight of each treatment was taken as the average of three cubic samples from each run. Each sample’s dimensions were measured using caliper and weighed subsequently. Pristine geopolymer samples (0% fiber loading, 0% H₂O₂ dosage, cured at 52.5°C) were measured to have a mean 2149.1 kg/m³ volumetric weight. The resulting volumetric weights of the samples ranged from 1966.38 kg/m³ to 2249.52kg/m³. The mean is 2099.687 kg/m³. The average value for the foamed samples is relatively high compared to that of a typical foam concrete whose volumetric weight are at most 1000kg/m³ [20]. Since the abaca fiber’s density is significantly lower than that of fly ash and other raw materials, it is reasonable for the composite’s volumetric weight to decrease with abaca loading. Likewise, increasing the foaming agent dosage reduced the volumetric weight due to formation of void spaces within the composite. Increasing the curing temperature also resulted to lower volumetric weight which could be due to higher moisture loss during curing.

Water absorption was measured following ASTM D570. The mass of a cubic sample from each run was measured. The samples were then submerged in distilled water for 24 hours, wiped dry at the surface before being weighed again. Volume changes were observably negligible throughout the experimental procedure. The mass percent moisture absorbed is taken as the water absorption, computed using Eq. 1.

$$WA = \frac{W_{sat} - W_{dry}}{W_{dry}} \times 100 \quad (1)$$

where WA = water absorption ; W_{sat} = mass at saturated state ; W_{dry} = mass at dry state

The pristine geopolymer sample’s measured water absorption value was 4.499%. The values ranged from 3.3821% to 13.9730% with a mean value of 6.6228%. The values measured for the experimental samples are found to be in the same range as reports on hardened OPC composites, which can range between 2-15%. A study of coir fiber-reinforced epoxy reported that higher fiber content resulted to increased water absorption due to the present hydroxyl groups [21]. In this study, however, the effect of the fiber loading was statistically insignificant to the composite’s water absorption. This is favorable since one of the main concerns of natural fiber reinforcement is the tendency for the organic fiber to draw water in due to its hydrophilic nature. The lack of significance of fiber loading effect to water absorption in this study suggests that the alkali treatment has sufficiently reduced the hydrophilic components in the fiber.

Measured volumetric weight and water absorption are summarized in **Table 3**.

Table 3. Volumetric weight and water absorption of composites

Fiber Loading (%)	H ₂ O ₂ Dosage (%)	Curing Temp. (°C)	Volumetric Weight (kg/m ³)	Water Absorption (%)
0	0.16	52.5	2249.52	4.26
0	0.32	52.5	2063.17	7.18
0	0.24	30	2178.76	13.97
0	0.24	75	2142.64	5.68
0.25	0.16	30	2155.76	8.95
0.25	0.16	75	2066.80	5.53
0.25	0.32	30	1986.12	5.25
0.25	0.32	75	2016.05	4.94
0.25	0.24	52.5	2190.26	3.26
0.5	0.16	52.5	2179.78	6.86
0.5	0.32	52.5	1966.38	7.09
0.5	0.24	30	2129.43	6.33
0.5	0.24	75	1976.08	6.78

3.4. Scanning electron microscopy (SEM) analysis of geopolymer composites

SEM images of selected samples at 2000x magnification are shown in **Fig. 4**.

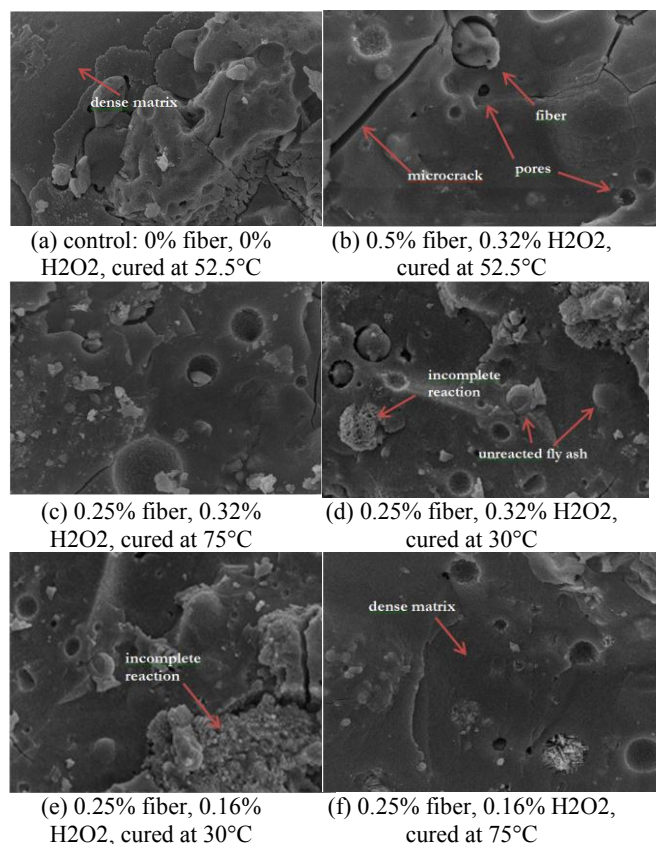


Fig. 4. SEM Images of geopolymer composites

SEM analysis can provide clues and qualitative validation of premises about the water absorption, and provide later on, the mechanical properties and thermal properties of the composite samples. Unreacted fly ash and incomplete reactions were observed largely in samples that were cured at low temperature as shown in **Fig. 4d** and **Fig. 4e**. Samples cured at higher temperatures formed more dense matrices, exhibiting less unreacted fly ash and incomplete reactions. Pores were visibly bigger and more evenly distributed in **Fig. 4c** and **Fig. 4f** which were cured at 75°C. Microcracks were also observed in most of the samples but were more evident in **Fig. 4b** and **Fig. 4c**. It can be observed in Figure 5.4b that the fiber-matrix gap seemed to have been the site for microcrack formation. In **Fig. 4d**, in which the sample was cured at low temperature, microcracks were not present along the abaca fibers. This verifies the premise that microcracks tend to form at high fiber loading and high curing temperature. Curing at low temperature, however, can result to incomplete reaction [22], as evidenced by **Fig. 4d** which shows more unreacted fly ash and less dense matrix. This can translate to lower strength, as well. Microcracks present in **Fig. 4c** could be due to the high H₂O₂ dosage and high curing temperature.

3.5. Mechanical properties of geopolymer composite

UNIFRAME stand-alone universal compression/flexural tester was used to measure the compressive and flexural strength of the samples. Compressive strength test was performed following ASTM C109. Meanwhile, the three-point flexural test (ASTM C348) was performed to calculate for the flexural strength of the composites.

3.5.1 Compressive strength of geopolymer composites

Compressive strength is a measure of the structure's resistance or ability to withstand compression stress. This parameter, which will be considered as a response in the experiment, is a key mechanical property for construction materials. Standard values of materials acceptable for use as structural 'residential concrete' are at least 17 MPa. Moreover, 28 MPa is the minimum compressive strength for materials finding application as commercial structures [23]. 50mm cubic samples were prepared, cured for 28 days and tested for compressive strength. In addition to the 13 treatments, a pristine geopolymer sample and 3 replicated treatments were prepared for the test. Samples were subjected to gradual load with rate 0.4 MPa/s. The maximum loads were recorded at failure. Three replicates were tested for each treatment. The mean ultimate load of the three replicates was taken as the compressive strength for each treatment. **Fig. 5** shows the set up for the compressive strength test.

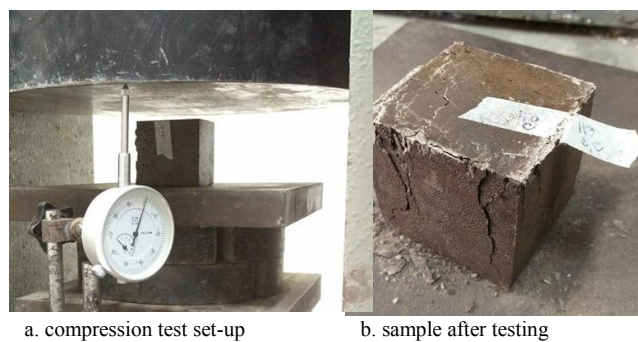


Fig. 5. Compressive strength test set-up

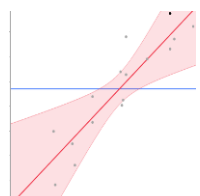
The average of the compressive strengths of three specimens was taken as the measured value for each run. Pristine geopolymer samples (0% fiber loading, 0% H₂O₂ dosage, cured at 52.5°C) were measured to have a mean compressive strength of 24.04 MPa. The compressive strength values ranged from 19.56 MPa to 36.85 MPa. The mean value is 29.26 MPa. Compressive strength requirements are at least 17 MPa and 28 MPa for residential and commercial concrete, respectively [24]. Compressive strength was analyzed as response to the three factors and a 2nd degree model was generated. The measured R² is 0.8275. **Table 4** and summarizes the compressive strength data. **Table 5** shows the ANOVA for compressive strength.

Table 4. Compressive strength of the abaca-reinforced geopolymer composites

Fiber Loading (%)	H ₂ O ₂ Dosage (%)	Curing Temp. (°C)	Compressive strength (MPa)
0	0.16	52.5	27.58
0	0.32	52.5	23.70
0	0.24	30	21.54
0	0.24	75	34.50
0.25	0.16	30	24.96
0.25	0.16	75	35.54
0.25	0.32	30	28.46
0.25	0.32	75	19.56
0.25	0.24	52.5	32.25
0.5	0.16	52.5	33.27
0.5	0.32	52.5	30.97
0.5	0.24	30	28.11
0.5	0.24	75	34.27
*0	0.24	75	2.23
*0.25	0.32	30	1.82
*0.5	0.16	52.5	2.96

*replicated treatments

Table 5. Compressive strength summary of fit and Analysis of Variance



Source	DF	Sum of Squares	Mean Square	F Ratio
Model	7	342.15	48.8788	6.8917
Error	8	56.74	7.0925	Prob > F
C. Total	15	398.89		0.0071

Table 6 summarizes the parameter estimates of the model for compressive strength. The abaca reinforcement was found to have improved the compressive strength of the composites. This signifies that the fibers have sufficiently been treated and have formed an effective interaction with the matrix. Foaming agent dosage expectedly decreases compressive strength since more voids are expected to form. Higher curing temperature also improved the compressive strength. This agrees with previous reports [19]. It is said that heat curing facilitates in the reaction and formation of dense geopolymer matrix. The interaction between H₂O₂ dosage and curing temperature, however, resulted to weaker composites. As evidenced by the SEM images and qualitative results of preliminary preparation of samples, it is likely due to the microcrack formation when H₂O₂ dosage and curing temperature are simultaneously set at high levels.

Table 6. Compressive strength model parameter estimates

Term	Estimate	Std Error	t Ratio	Prob> t
Intercept	32.220605	1.723139	18.7	<.0001
Fiber(0,0.5)	2.5907439	0.899289	2.88	0.0182
H2O2(0.16, 0.32)	-2.663281	0.901261	-2.96	0.0161
CT(30,75)	2.7500156	0.901261	3.05	0.0138
H2O2*CT	-4.752168	1.277011	-3.72	0.0048

Fiber - % Fiber Loading; H2O2 - % H₂O₂ Dosage; CT - Curing Temperature °C

3.5.2 Flexural strength of geopolymer composites

Flexural strength, which is also referred to as bend strength, is the mechanical property which measures the stress in the material right before it yields or deforms in a bending test. It is the highest stressed loaded to the material at point of failure. Foam concrete's flexural stress was typically measured to be in the range 15% to 35% of its own compressive strength [25]. Very few studies have considered this parameter. A specimen with dimensions 40x40x160-mm was prepared from each treatment for this test. The test was performed after 28 days of curing. Each sample was subjected to rate of load 0.3 MPa/s; flexural strength was calculated following ASTM C348. **Fig. 6** shows the set up for flexural test.



Fig. 6. Flexural strength test set-up

A pristine geopolymer sample (0% fiber loading, 0% H₂O₂ dosage, cured at 52.5°C) was measured to have 5.81 MPa flexural strength. As shown in **Table 7**, the flexural strength values ranged from 2.415 MPa to 6.254 MPa, with a mean value of 4.323 MPa. These values are in the same range as previous reports on geopolymer's flexural strength [26-27]. **Table 7** summarizes the measured flexural strength for each treatment.

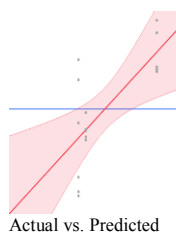
Table 7. Flexural strength of the abaca-reinforced geopolymer composites

Fiber Loading (%)	H ₂ O ₂ Dosage (%)	Curing Temp. (°C)	Flexural Strength (MPa)
0	0.16	52.5	6.25
0	0.32	52.5	4.23
0	0.24	30	5.39
0	0.24	75	2.41
0.25	0.16	30	5.18
0.25	0.16	75	5.98
0.25	0.32	30	3.70
0.25	0.32	75	3.87
0.25	0.24	52.5	4.95
0.5	0.16	52.5	5.23
0.5	0.32	52.5	3.84
0.5	0.24	30	4.01
0.5	0.24	75	2.82
*0	0.24	75	2.51
*0.25	0.32	30	3.64
*0.5	0.16	52.5	5.13

*replicated treatments

A second-degree model was fit with the data, and R² = 0.5362. The model itself was not very significant as shown in **Table 8**. The table summarizes the model's fit and ANOVA for flexural strength.

Table 8. Flexural strength summary of fit and Analysis of Variance



Source	DF	Sum of Squares	Mean Square	F Ratio
Model	2	11.17650	5.58825	7.5135
Error	13	9.668871	0.74376	Prob > F
C. Total	15	20.84537		0.0068

Among the factors, foaming agent dosage was found to be a significant factor, which expectedly caused flexural strength to decline due to formation of void spaces in the matrix. This relationship was observed from Table 9, which shows the parameter estimates of the model.

Table 9. Compressive strength model parameter estimates

Term	Estimate	Std Error	t Ratio	Prob> t
Intercept	3.6819481	0.352079	10.46	<.0001
H2O2 (0.16,0.32)	-0.850624	0.27272	-3.12	0.0081
H2O2*H2O2	1.0251364	0.445349	2.3	0.0385

H2O2 – % H₂O₂ Dosage

The negative coefficient associated with the first-degree factor H₂O₂ (foaming agent dosage) signifies increasing H₂O₂ dosage results to lower flexural strength. However, the model generated has found significance in the second-degree factors of the H₂O₂ dosage. Intriguingly, the second-degree parameter was associated with a positive coefficient. This signifies that a curve exists and that the flexural strength can possibly increase at a threshold H₂O₂ dosage. The voids and pores formed from added foaming at an optimal or desired dose, can possibly serve as a “shock absorber” during impact. This could explain how foaming can improve flexural strength as suggested by the positive coefficient associated with this parameter.

In this study, the effect of natural fiber reinforcement to flexural strength remained inconclusive. Although statistical analysis presents no indication of any significant effect of fiber reinforcement to flexural strength, it was qualitatively observed that samples subjected to bending load were somehow held together by the fibers at the point of failure, as shown in **Fig. 7**.



Fig. 7. Bridging fibers at composite's point of failure

4 Conclusions

Treated fibers appeared rougher and more uniform in SEM images; this, in theory, facilitated in interlocking of fiber with the matrix and could therefore enhance the composite's performance. The alkali treatment has sufficiently removed hydrophilic components and impurities as evidenced by TGA results and the lack of significance of fiber loading's effect on the composite's water absorption.

Compressive strength of the samples ranged from 19.56 MPa to 36.85 MPa. The mean value is 29.26 MPa – comparable to the standards for residential and commercial structural concrete. Abaca reinforcement and heat curing both improved the compressive strength. Foaming resulted to weaker composites. The interaction of H₂O₂ dosage and curing temperature significantly affected compressive strength. Compressive strength declined when these factors are set at high levels at the same time due to microcrack formation as observed in the samples' SEM images.

Flexural strength values ranged from 2.415 MPa to 6.254, with a mean value of 4.323 MPa. Addition of foaming agent was observed to weaken the composite's flexural strength, as expected. The correlation of the factors to flexural strength remains inconclusive due to the model's lack of fit. Fiber aggregation during the hardening period could have contributed to the experimental errors. It was, however, qualitatively observed that the abaca fibers bridged across the point of failure during the performance of the flexural test.

References

1. L. Perez-Lombard, J. Ortiz, C. Pout. *Energy Build.* **40**, 394-398 (2008)
2. Z. Zhang, J.L. Provis, A. Reid, H. Wang. *Cem. Concr. Compos.* **62**, 97-105 (2015)
3. M.W. Ibrahim, N. Jamaludin, J. Irwan, P. Ramadhansyah, A.S. Hani. *AMR.* **911**, 489-493 (2014)
4. S. Taj, M. Munawan, S. Khan. *Proceedings of the Pakistan Academy of Sciences.* **44**(2), 129-144 (2007).
5. Philippine Statistics Authority. Selected Statistics on Agriculture 27, 13-18 (2016) Retrieved May 6, 2017, from <https://psa.gov.ph/sites/default/files/Selected%20Statistics%20on%20Agriculture%202016.pdf>
6. R. Dungani, M.S. Karina, A. Sulaeman, D. Hermawan, A. Hadiyane. *Asian J. Plant Sci.* **15**(1), 42-55 (2016).
7. R. Araral. Turning Abaca Wastes Into Export Grade Handicraft (2004) Retrieved August 13, 2017, from http://sntpost.stii.dost.gov.ph/frames/OctToDec04/pg41_exportGradehandicraft.htm
8. C. Feliciano. Abaca shipments up nearly 40% by value in 11 months to November. (2015). Retrieved on August 13, 2017 from <http://www.bworldonline.com/content.php?section=Economy&title=abaca-shipments-up-nearly-40%-by-value-in-11-months-to-november&id=106608>
9. J. Arcalas. PHL abaca production grew 5.7% in 2016. (2017). Retrieved August 13, 2017 from <http://www.businessmirror.com.ph/phl-abaca-production-grew-5-7-in-2016/>
10. E. Agung, S. Sapuan, M. Hamdan, H.D. Zaman, U. Mustofa. *Int. J. Phys. Sci.* **6**(8), 2100-2106 (2011)
11. G. Islam, S. Gupta. *Int. J. Sust. Built Environ.* **5**(2), 345-354 (2016)
12. P. Ramadevi, D. Sampathkumar, B. Bennehalli, P. Badyankal, S. Venkateshappa. *Int. J. Chem.* **35**(2), 1699-1706 (2014)
13. O. Faruk, A. Bledzki, H. Fink, M. Sain. *Prog. Polym. Sci.* **37**(11), 1552-1596 (2012)
14. P. Ramadevi, S. Venkateshappa, R. Sampathkumar, D. Bennehalli. *Bioresour.* **7**(3), 3515-3524 (2012)
15. A. Jabbar, J. Militký, J. Wiener, M.U. Javaid, S. Rwwaire. *Indian J. Fibre Text. Res.* **41**, 249-254 (2016)
16. O. Onuaguluchi, N. Banthia. *Cem. Concr. Compos.* **68**, 96-108 (2016).
17. M. Cai, H. Takagi, A.N. Nakagaito, Y. Li, G.I. Waterhouse. *Composites Part A.* **90**, 589-597 (2016)
18. M.M. Kabir, H. Aravinthan, H. Wang, T. Cardona, K.T. Lau. *Energy, Environment and Sustainability. EddBE2011 Proceedings.* 2011, 94-99 (2011)
19. J. Zhang, L. Feng, D. Wang, R. Zhang, G. Liu, G. Cheng. *Bioresour. Technol.* **153**, 379-382 (2014)
20. V. Ducman, L. Korat. *Mater. Charact.* **113**, 207-213 (2016)
21. G. Das, S. Biswas. *Mater. Sci. Eng.* **115**(2016)
22. M. Abdullah, K. Hussin, M. Bnhussain, K. Ismail, Z. Yahya, R. Razak. *Int. J. Mol. Sci.* **13**(2012)
23. M. Jones, A. Mccarthy. *Fuel.* **84**(11), 1398-1409 (2005)
24. National Ready Mixed Concrete Association [NRMCA]. *Concrete in Practice* (2003). Retrieved June 29, 2017, from http://welschreadymix.com/wp-content/uploads/2016/04/CIP35-Testing_Compressive_Strength_of_Concrete.pdf
25. Y. Amran, N. Farzadnia, A.A. Ali. *Constr. Build. Mater.* **101**, 990-1005 (2015)
26. K. Korniejenko, E. Frączek, E. Pytlak, M. Adamski. *Procedia Engineering.* **151**, 388-393 (2016)
27. A. Bhutta, P.H. Borges, C. Zanotti, M. Farooq, N. Banthia. *Cem. Concr. Compos.* **80**, 31-40 (2017)